Eur. Phys. J. D **37**, 67–74 (2006)
DOI: 10.1140/epjd/e2005-00257-7

THE EUROPEAN PHYSICAL JOURNAL D

Electron impact total and ionization cross-sections for some hydrocarbon molecules and radicals

M. Vinodkumar[1,2], K.N. Joshipura[3], C.G. Limbachiya[3,4], and B.K. Antony[5,a]

[1] Department of Physics and Astronomy, Open University, Milton Keynes MK7 6AA, UK
[2] VP & RPTP Science College, Vallabh Vidyanagar, 388120 Gujarat, India
[3] Department of Physics, Sardar Patel University, Vallabh Vidyanagar, 388120 Gujarat, India
[4] PS Science College, Kadi (N.G.), 382715 Gujarat, India
[5] Department of Environmental, Earth & Atmospheric Sciences, University of Massachusetts Lowell, 265 Riverside Street, Lowell, MA 01854-5045, USA

Received 8 January 2005 / Received in final form 15 July 2005
Published online 27 September 2005 – © EDP Sciences, Società Italiana di Fisica, Springer-Verlag 2005

Abstract. Electron impact total (50 to 2000 eV) and ionization (threshold to 2000 eV) cross-sections are calculated using the SCOP and CSP-ic methods [Phys. Rev. A **69**, 022705 (2004)] for the hydrocarbon molecules (CH_4, C_2H_2, C_2H_4, C_2H_6, C_3H_4, C_3H_6 and C_3H_8) and radicals (CH_x ($x = 1{-}3$)). Present method has already been tested successfully to many other aeronomic [Int. J. Mass Spectrom. **233**, 207 (2004)] and plasma molecules and radicals. Our results exhibited in this paper show good agreement with experimental results where available. For the radical species, we have presently done a first estimate of the total cross-sections.

PACS. 34.80.Bm Elastic scattering of electrons by atoms and molecules – 34.80.Gs Molecular excitation and ionization by electron impact

1 Introduction

For the last few decades the importance and applications of hydrocarbons are increasing in molecular chemistry and plasma physics. They play dominant role in edge processes of magnetically confined high temperature hydrogen plasma [1]. These molecules are also important constituents in various astrophysical environments [2,3]. The knowledge of electron impact ionization cross-sections for ethane is useful in understanding the fundamental processes of the energy deposition in biological cells and energy transfer in gases used in dosimetry.

Total cross-sections (TCS) for electron scattering from atoms and molecules provide useful insight in verifying and testing various models of electric and magnetic interactions. Electron induced ionization cross-sections and probabilities of other processes like excitations in molecules determine the density and reactivity of low temperature technological plasmas. Along this line of investigation, the electron as well as positron induced processes, including ionization as a dominant inelastic channel at intermediate and high energies, play important roles in plasma-processing, aeronomy and in biological systems and other environmental sciences. Moreover, in order to develop understanding of the basic chemical behaviour of above listed hydrocarbons, the data regarding the total elastic, inelastic and ionization cross-sections would prove crucial and therefore such study has attracted many theoreticians and experimentalists in last few decades. However not much theoretical data is available for the total and ionization cross-sections for C_3H_4, C_3H_6, and C_3H_8 molecules [4].

In this paper we have reported the total cross-section, Q_T and total ionization cross-section, Q_{ion} for C_2H_2, C_2H_4 C_2H_6 C_3H_4, C_3H_6 and C_3H_8 molecules and CH_x ($x = 1{-}3$) radicals by electron impact. For the standard target CH_4 our results are included for comparison.

Calculations of complete TCS Q_T for C_2H_2, C_2H_4 and C_2H_6 molecules are scarce, but there is a considerable experimental study on these molecules. For C_2H_2, Ariyasinghe and Powers [5], Xing et al. [6] and Sueoka and Mori [7] have measured Q_T and corresponding theoretical values were reported by Jain and Baluja [8]. The total ionization cross-section, Q_{ion} are calculated by many groups [9–11], while experimentally it has been measured by Hayashi [12]. The Q_T for C_2H_4 molecule is measured by Sueoka and Mori [13] and Ariyasinghe and Powers [5] and the theoretical values are reported by Jain and Baluja [8] and Jiang et al. [14]. There are extensive measurements [12,15,16] for Q_{ion}, while the only theoretical results are due to Hwang et al. [17]. For C_2H_6 molecule the measurements of Q_T are reported by Hayashi [18] and Ariyasinghe and Powers [5], but no theoretical data has

---

[a] e-mail: `bk_antony@rediffmail.com`

been reported in this case. The Q_{ion} have been measured by Nishimura and Tawara [16], Chatham et al. [19] and Schram et al. [20], while theoretical data are due to BEB method of Kim [21].

C_3H_4, C_3H_6 and C_3H_8 targets are less investigated both theoretically and experimentally. There is no theoretical data on Q_T for C_3H_4, but the experimental results are reported by Makochekanwa et al. [22] and Szmytkowski and Kwitnewski [23]. However, no calculations or measurements are reported on Q_{ion} for this molecule. Q_T for C_3H_6 molecule were measured by Floeder et al. [24] and Nishimura and Tawara [25], whereas Q_{ion} were measured by Nishimura and Tawara [16] and Schram et al. [20] and calculated by Deutsch et al. [26]. Finally for C_3H_8 molecule, there are measurements for Q_T [23,24,27], but no theoretical data is reported. The Q_{ion} of C_3H_8 have been measured by [16,20], and theoretical results were reported by [17].

The transient radicals pose difficulties in the cross-section measurements due to their high reactivity and less stability. Hence the experimental results need to be supplemented through alternative theoretical models. Besides, none of the previous theories discuss ionization in relation to processes like elastic scattering and inelastic collisions like excitation by electron impact. In this work we have also reported calculations on Q_T and Q_{ion} for CH_x radicals. Comparisons are available only for Q_{ion} from the experiments of Tarnovsky et al. [28], Baiocchi et al. [29] and from the BEB calculations [21]. Preliminary estimates for CH_x radicals were given in our earlier paper [30].

Our present aim is to find the total elastic and inelastic cross-sections by Spherical Complex Optical Potential (SCOP) method. The total cross-section, Q_T can be obtained as,

$$Q_T(E_i) = Q_{el}(E_i) + Q_{inel}(E_i). \tag{1}$$

Here, the first term is the total elastic cross-section and the second term is the total inelastic cross-section. This does not incorporate the non-spherical effects, e.g. the dipole rotation, which are not significant in the present energy range, but may be added to Q_T for the polar molecules [31]. Then by applying the CSP-ic (complex scattering potential-ionization contribution) method we have derived Q_{ion} from Q_{inel}. Our approach is discussed briefly in the next section and comparison of the present results is made with available experimental and theoretical data in Section 3.

2 Theoretical methodology

We explain in brief the theoretical formalism employed to determine the Q_T and Q_{ion} for the impact of electrons on the molecules and radicals studied. A detailed description can be found from our earlier papers [32–34] and references therein. The present calculations are based on the spherical complex scattering potential $V_{opt} = V_R + iV_I$, where V_R and V_I are the real and imaginary parts of the total potential V_{opt} as discussed in our recent papers [31–36]. We employ this central potential in to the Schrödinger equation to calculate the total cross-sections of simultaneous elastic and inelastic scattering of electrons. For this purpose a local absorption potential V_{abs} [37] is constructed appropriately, by treating the quantity Δ appearing in the absorption potential as energy dependent parameter [32,33] to account for electronically inelastic scattering. The modified potential is employed as the imaginary part of the total potential V_{opt} to calculate the total inelastic cross-section Q_{inel}. The inelastic cross-section Q_{inel}, which is a quantity not accessible directly in experiments, can be partitioned basically as,

$$Q_{inel}(E_i) = \Sigma Q_{exc}(E_i) + Q_{ion}(E_i). \tag{2}$$

In equation (2), the first term is the sum of the total excitation cross-sections for all the accessible electronic transitions. These transitions are dominated by low-lying dipole allowed states, for which the thresholds lie below the ionization energy. The second term stands for all the allowed ionization processes in the targets by electron impact. Now, the ionization corresponds to infinitely many open channels, so that as incident energy increases above the ionization threshold, the cross-section Q_{ion} provides the major contribution to the theoretical quantity Q_{inel}, and therefore,

$$Q_{inel}(E_i) \geq Q_{ion}(E_i). \tag{3}$$

Thus we find that Q_{inel} contains Q_{ion}. The latter cannot be projected out rigorously from the former cross-section. To do this approximately we have introduced [31] an energy dependent function defined as,

$$R(E_i) = \frac{Q_{ion}(E_i)}{Q_{inel}(E_i)} \tag{4}$$

where, we must have $R = 0$ for $E_i \leq I$, and $0 \leq R \lesssim 1$, for $E_i > I$ in view of equation (3). A first theoretical estimate of the ratio R (Eq. (4)) was given by Turner et al. [38], who had found $R \cong 0.65$ above 100 eV. In our approach called 'Complex Scattering potential-ionization contribution' (CSP-ic) method [31–34], we determine this ratio in the following analytical form,

$$R(E_i) = 1 - C_1 \left[\frac{C_2}{U + a} + \frac{\ln(U)}{U} \right] \tag{5}$$

where U is the dimensionless variable defined through, $U = E_i/I$. The above expression involves three parameters C_1, C_2 and a, which are determined from the three conditions on the function $R(E_i)$, vide [31–34]. Determination of these parameters is based on the general observation that typically around $E_i = 100$ eV when Q_{ion} for a molecule reaches its maximum, its contribution to Q_{inel} is about 70 to 80% in most of the atomic-molecular systems. This can be basically attributed to infinitely many scattering channels offered by the continuum in contrast with a finite number of important discrete electronic excitations. Having thus determined $R(E_i)$, we evaluate Q_{ion}

Table 1. Q_T and Q_{ion} for molecular hydrocarbons (in Å^2 and E_i in eV).

E_i	CH_4		C_2H_2		C_2H_4		C_2H_6		C_3H_4		C_3H_6		C_3H_8	
	Q_T	Q_{ion}	Q_T	Q_{ion}	Q_T	Q_{ion}	Q_T	Q_{ion}	Q_T	Q_{ion}	Q_T	Q_{ion}	Q_T	Q_{ion}
15	–	0.17	–	0.68	–	0.27	–	0.16	–	0.61	–	0.6	–	1.25
20	–	0.85	–	1.48	–	1.22	–	1.12	–	1.43	–	2.05	–	2.77
30	–	2.12	–	2.67	–	3.17	–	3.48	–	2.87	–	4.59	–	5.54
40	–	3	–	3.54	–	4.43	–	5.07	–	4.19	–	6.02	–	7.45
50	13.2	3.48	13.3	4.06	15.9	5.11	17.3	5.97	17.6	5.06	19.4	6.76	22.5	8.3
60	11.9	3.71	11.9	4.34	14.4	5.38	16.4	6.34	16.5	5.57	18.5	7.09	20.9	8.59
70	10.8	3.81	10.9	4.46	13.2	5.43	15.6	6.38	15.7	5.79	17.6	7.08	19.5	8.7
80	9.93	3.84	10.1	4.47	12.3	5.38	14.9	6.26	14.9	5.83	16.8	6.94	18.4	8.68
90	9.23	3.84	9.5	4.43	11.5	5.29	14.2	6.09	14.2	5.78	16.1	6.76	17.1	8.56
100	8.64	3.81	8.98	4.33	10.9	5.16	13.5	5.91	13.5	5.7	15.6	6.64	15.9	8.41
150	6.65	3.48	7.23	3.77	8.81	4.48	11.4	4.99	11.4	5.32	12.8	5.95	12.7	7.45
200	5.47	3.01	6.19	3.3	7.54	3.95	9.87	4.33	9.87	4.86	11.2	5.39	10.8	6.68
300	4.08	2.4	4.94	2.64	6.01	3.18	8.91	3.44	8.19	4.11	9.41	4.58	8.72	5.43
400	3.28	2.04	4.18	2.2	5.07	2.67	7.06	2.88	7.13	3.56	8.18	3.99	7.43	4.66
500	2.75	1.72	3.65	1.89	4.41	2.31	6.21	2.47	6.35	3.14	7.27	3.54	6.55	4.11
600	2.37	1.51	3.25	1.64	3.92	2.03	5.52	2.17	5.73	2.81	6.54	3.18	5.86	3.66
700	2.09	1.33	2.94	1.47	3.54	1.82	5.02	1.94	5.23	2.54	5.95	2.9	5.49	3.33
800	1.87	1.21	2.69	1.33	3.24	1.64	4.52	1.75	4.81	2.33	5.47	2.65	5.1	3.03
900	1.68	1.1	2.48	1.21	2.98	1.5	4.11	1.6	4.45	2.14	5.05	2.45	4.78	2.85
1000	1.54	1.01	2.31	1.11	2.77	1.38	3.81	1.47	4.15	1.99	4.7	2.27	4.4	2.63
1500	1.05	0.66	1.72	0.8	2.06	0.98	2.67	1.06	3.09	1.45	3.48	1.67	3.43	1.98
2000	0.7	0.43	1.39	0.63	1.65	0.78	2.11	0.82	2.46	1.13	2.75	1.31	2.65	1.64

from our calculated Q_{inel} through equation (4). Although this constitutes a semi empirical approximation, the reliability and accuracy of our method has been tested adequately in a variety of molecules in gas phase, as discussed in our recent papers [32–34]. The CSP-ic method satisfactorily predicts the position and magnitudes of the peak of the total ionization cross-sections, which have a dependence on the threshold value, size and number of electrons of the target molecule.

The present method employs two of the most well known target properties as the basic inputs viz. (i) The first ionization energies and (ii) the molecular geometries (bond lengths, bond angle etc.). Our method provides a useful alternative approach to the current theories viz., BEB [39], siBED [40] and the DM [41].

3 Results and discussion

The present Q_T and Q_{ion} results on stable and radical species of some hydrocarbons are discussed here. Calculated results for these target are tabulated in Tables 1 and 2. Comparisons are made graphically in the coming sections.

Table 2. Q_T and Q_{ion} for hydrocarbon radicals (in Å^2 and E_i in eV).

E_i	CH		CH_2		CH_3	
	Q_T	Q_{ion}	Q_T	Q_{ion}	Q_T	Q_{ion}
15	-	0.38	-	0.28	-	0.32
20	-	0.88	-	0.72	-	0.91
30	-	1.54	-	1.56	-	1.81
40	-	1.95	-	2.09	-	2.53
50	8.67	2.2	12.6	2.37	11.7	2.90
60	7.93	2.32	11.8	2.49	10.7	3.07
70	7.33	2.34	11.1	2.53	9.96	3.13
80	6.85	2.34	10.4	2.53	9.31	3.15
90	6.43	2.31	9.86	2.51	8.77	3.12
100	6.08	2.25	9.35	2.47	8.29	3.06
150	4.83	1.91	7.47	2.17	6.60	2.66
200	4.04	1.65	6.26	1.88	5.52	2.31
300	3.08	1.32	4.76	1.49	4.21	1.83
400	2.50	1.09	3.86	1.22	3.42	1.51
500	2.11	0.93	3.26	1.04	2.89	1.29
600	1.83	0.81	2.82	0.91	2.50	1.14
700	1.62	0.71	2.49	0.80	2.21	1.01
800	1.46	0.64	2.23	0.72	1.99	0.91
900	1.32	0.58	2.03	0.64	1.80	0.84
1000	1.22	0.53	1.86	0.58	1.65	0.75
1500	0.86	0.33	1.31	0.37	1.18	0.50
2000	0.68	0.24	1.01	0.25	0.91	0.36

3.1 Stable molecules

3.1.1 CH_4

Methane is nearly spherical, such that rotational excitation is weak. Hence this is a perfect case suitable to our theory and is included here as a standard hydrocarbon target. As the Figure 1 shows the present total (complete) cross-sections Q_T of methane are in a good agreement with the theoretical values of Jain and Baluja [8], and also with the measurements of Zecca et al. [42]. The theoretical

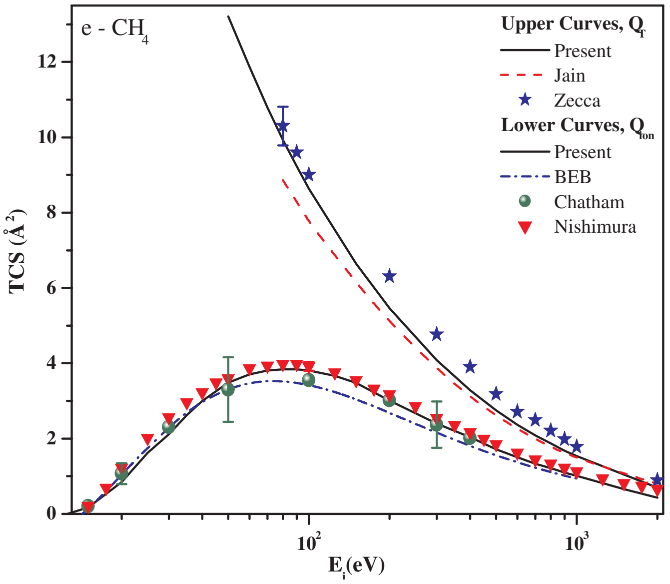

Fig. 1. Q_T and Q_{ion} for CH_4 molecule. $Q_T \rightarrow$ solid curve – present; dash – Jain [8]; star – Zecca [42]. $Q_{ion} \rightarrow$ solid curve – present; dash-dot – BEB [21]; circle – Chatham [19]; inverted triangle – Nishimura [16].

values of Lee et al. [43] (not shown here) seem to be in agreement with the present theory up to about 200 eV. The ionization cross-sections for methane reach a peak at about 70 eV. The Q_{ion} derived in our CSP-ic approach are in very good accord with the BEB theory [21] and the measured data of Chatham et al. [19] and Nishimura and Tawara [16]. Measurements of Chatham et al. have an uncertainty of about 10% and Nishimura and Tawara of 5%. The Q_T and Q_{ion} for CH_4 along with its radicals are also exhibited in Table 1.

3.1.2 C_2H_2

In this and remaining cases, we have used the multi-centre approximation method (group additivity method) [44,45] to calculate Q_T and Q_{ion} for all other stable molecules. In this method, the cross-sections for different groups in a molecule were calculated separately by the single centre approach and then added together to get the total cross-section of the molecule. In C_2H_2, for example, the group CH is considered as a unit for additivity. The justification for group additivity comes from relatively larger C–C bond length in all these molecules.

The upper curves in Figure 2 show our Q_T for C_2H_2 compared with the theory of Iga et al. [46] and experiments of Ariyasinghe and Powers [5] and Sueoka [7]. Over most of the energy range our results are in agreement with measurements and the theoretical data. The lower curve in Figure 2 exhibits Q_{ion} for C_2H_2. The present results are in excellent agreement with the BEB theory [21] and measurements of Hayashi [12] and Gaudin and Hagemann [11], well within an uncertainty of about 10%. Experimental values of Zheng and Srivastava [10] (not shown here) are above all these plotted Q_{ion} curves.

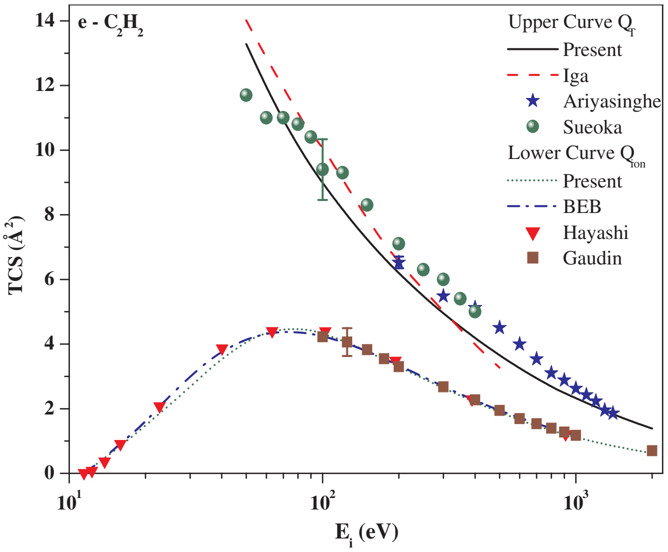

Fig. 2. Q_T and Q_{ion} for C_2H_2. $Q_T \rightarrow$ solid curve – present; dash – Iga [46]; star – Ariyasinghe [5]; circle – Sueoka [7]. $Q_{ion} \rightarrow$ dotted curve – present; dash-dot – BEB [21]; inverted triangle – Hayashi [12]; square – Gaudin [11].

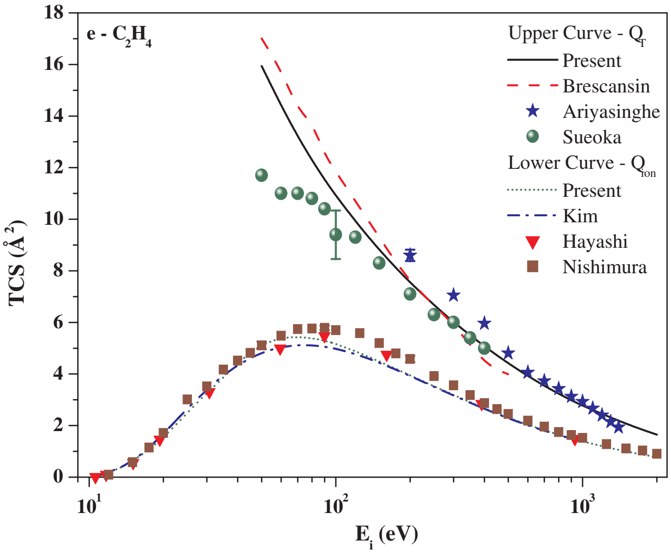

Fig. 3. Q_T and Q_{ion} for C_2H_4. $Q_T \rightarrow$ solid curve – present; dash – Brescansin [47]; star – Ariyasinghe [5]; circle – Sueoka [7]. $Q_{ion} \rightarrow$ dotted curve – present; dash-dot – BEB [21]; inverted triangle – Hayashi [12]; square – Nishimura [16].

3.1.3 C_2H_4

In Figure 3, the present TCS for C_2H_4 are displayed. The upper curves give our Q_T along with the experiments [5,47]. The theoretical values of Brescansin et al. [47] show a behaviour with respect to our values, similar to that of Iga et al. in C_2H_2. The present Q_{ion} curve (lower) in Figure 3 is in nice agreement with the BEB theory [21] and experimental data [12,16]. Values of [16] are slightly higher, but our present results are within their experimental uncertainty of 5%. Older measurement of

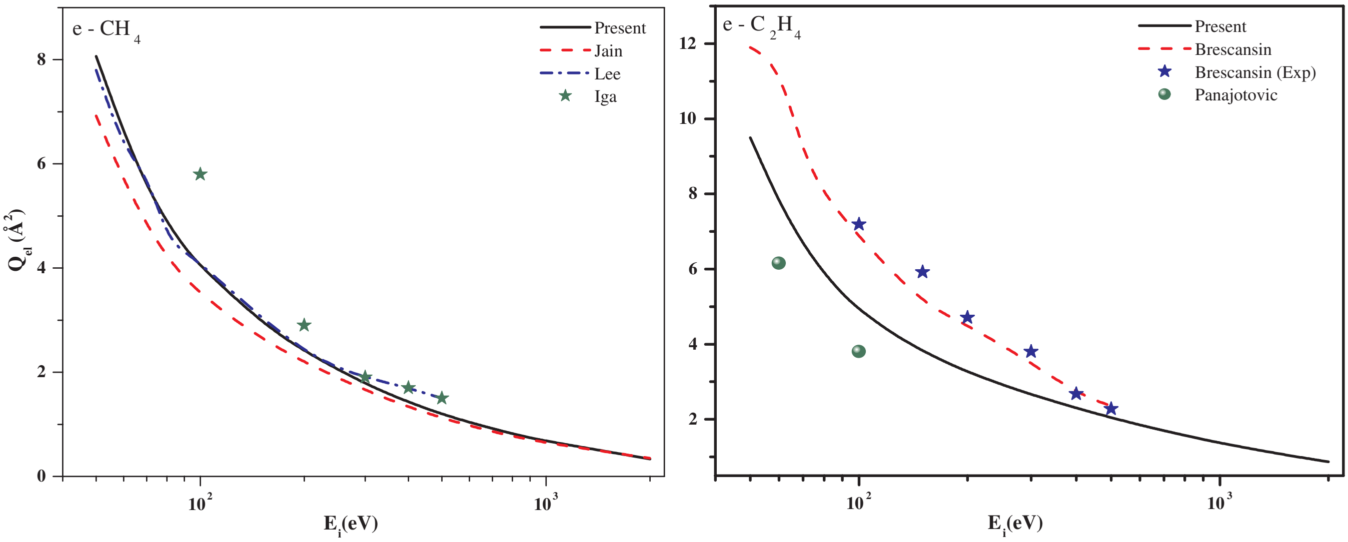

Fig. 4. Q_{el} for CH_4 and C_2H_4 molecules. *e*–CH_4 → solid curve – present; dash – Jain [8]; dash-dot – Lee [43]; star – Iga [46]. *e*–C_2H_4 → solid curve – present; dash – Brescansin [47]; star – Brescansin (Exp) [47]; filled circle – Panajotovic [48].

Rapp and Englander-Golden [15] (not shown here) seem to overestimate the Q_{ion} presented here.

The present calculations also yield total elastic cross-sections Q_{el}, hence sample comparisons for this quantity have been given in Figure 4. While CH_4 case (Fig. 4a) shows a good general agreement, there are differences among the different results in the case of C_2H_4 (Fig. 4b). For the sake of brevity we have not included the Q_{el} for other targets, but the values are available with the authors.

3.1.4 C_2H_6

Total and ionization cross-sections for non-polar C_2H_6 are plotted in Figure 5. The upper curves in Figure 5, compare the present Q_T for C_2H_6 with the measurements [5,13]. Even though our results are slightly above these values, they fall within the experimental uncertainty and the general shape is preserved throughout the energy range. The lower curves in Figure 5 show the comparison of present Q_{ion} for C_2H_6 with the BEB theory [21] and the experimental results [16,18,19]. Up to the peak of ionization, our values are in excellent agreement with these data, after which our values are slightly lower but still close to the experiments.

3.1.5 C_3H_4

For the exotic target C_3H_4 (Allene), the Q_T and Q_{ion} are plotted in Figure 6. The present Q_T on C_3H_4 are in general agreement with the experiments of Makochekanwa et al. [22], within their experimental uncertainties. However, the measurement of Szmytkowski et al. [23] overestimates and shows a behaviour different from other results. We must note that towards lower energies the non-spherical interactions enhance the total cross-sections Q_T.

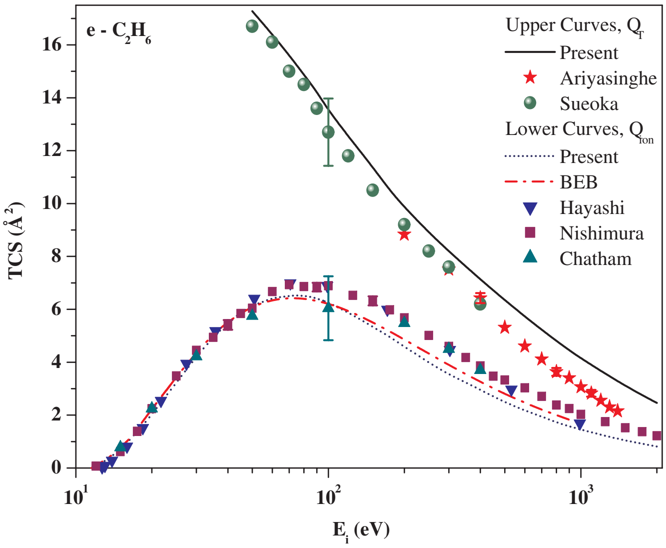

Fig. 5. Q_T and Q_{ion} for C_2H_6. Q_T → solid curve – present; star – Ariyasinghe [5]; circle – Sueoka [13]. Q_{ion} → dotted curve – present; dash-dot – BEB [21]; inverted triangle – Hayashi [18]; square – Nishimura [16]; triangle – Chatham [19].

In case of Q_{ion} of the present target, currently there are no other experimental or theoretical data available for this molecular species. Our results have retained expected nature and provide the first hand data for this target.

3.1.6 C_3H_6

In Figure 7 the upper curves exhibit the present Q_T for C_3H_6 with the experiments of Floeder et al. [24] and Nishimura and Tawara [25]. Present values are in good agreement with the results of Floeder et al. [24], but the measurement of Nishimura and Tawara [25] are on higher

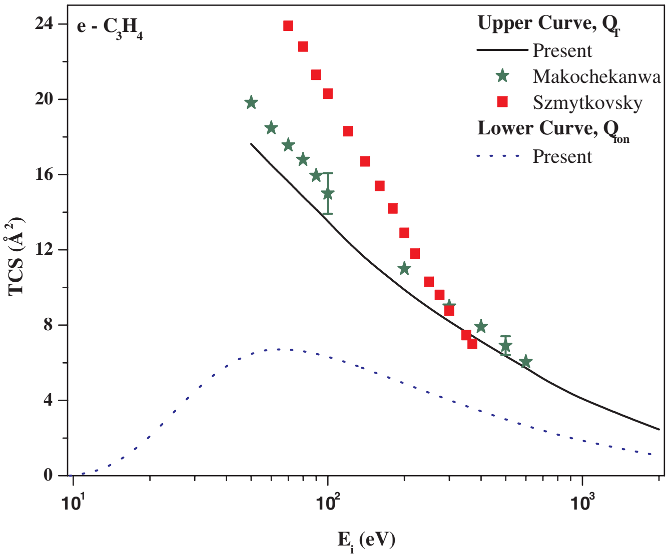

Fig. 6. Q_T and Q_{ion} for C_3H_4. Q_T → solid curve – present; star – Makochekanwa [22]; square – Szmytkowski [23]. Q_{ion} → dotted curve – present.

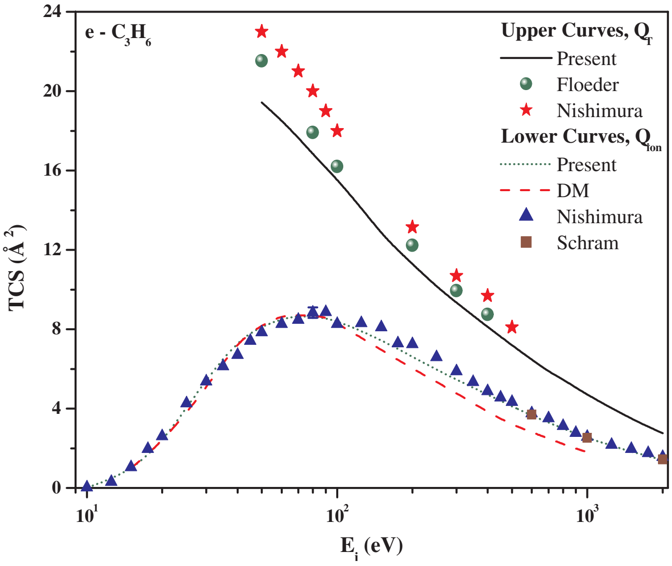

Fig. 7. Q_T and Q_{ion} for C_3H_6. Q_T → solid curve – present; circle – Floeder [24]; star – Nishimura [25]. Q_{ion} → dotted curve – present; dash – DM [26]; triangle – Nishimura [16]; square – Schram [20].

side at lower energies. They tend to approach each other with increase in energy.

The lower curves display the Q_{ion} which match reasonably well with the DM theory [26] till the peak and with the measurements of Nishimura and Tawara [16] and Schram et al. [20]. The DM theory [26] seems to underestimate after the peak of Q_{ion}. We have pointed out this behaviour in our earlier work too [34]. The experimental values of Nishimura and Tawara [16] are slightly higher than our calculated results. However, present results are in satisfactory agreement with the old work of Schram et al. [20], within an uncertainty of 11%.

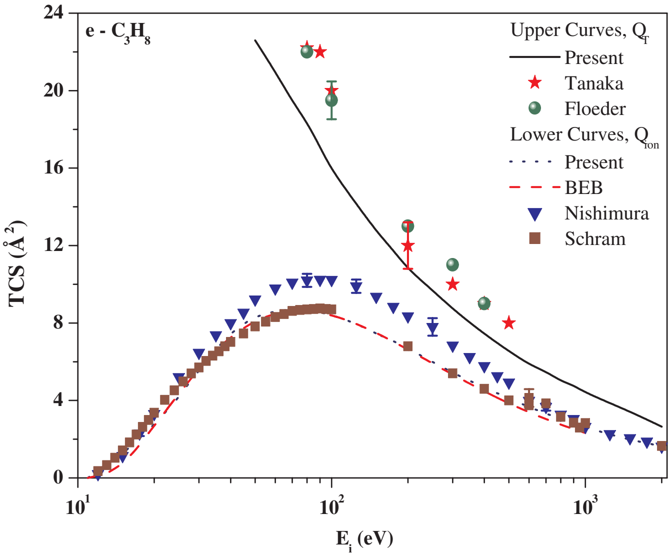

Fig. 8. Q_T and Q_{ion} for C_3H_8. Q_T → solid curve – present; star – Tanaka [27]; circle – Floeder [24]. Q_{ion} → dotted curve – present; dash-dot – BEB [21]; inverted triangle – Nishimura [16]; square – Schram [20].

3.1.7 C_3H_8

In Figure 8 we present our results on C_3H_8. Here Q_T curves are shown with the measurements of Tanaka et al. [27] and Floeder et al. [24]. Our calculated Q_T are lower than these results, but display similar energy dependence throughout. For the Q_{ion} of C_3H_8, our values are in good agreement with the BEB theory [21], but slightly lower than the measurements of Nishimura and Tawara [16] at the peak of Q_{ion}. An old measurement of Schram et al. [20] at high energy region is closer to our values.

3.2 Radicals

The transient radicals CH_x ($x = 1$–3) are difficult to examine experimentally. The present results of Q_T and Q_{ion} from CH, CH_2 and CH_3 hydrocarbon radicals are exhibited in Figures 9–11. The upper curves on all these graphs show Q_T and lower curves show Q_{ion}.

3.2.1 CH, CH_2 and CH_3

As shown in Figures 9, 10 and 11, our present theory yields ionization cross-sections that are in good agreement with the BEB theory of Ali et al. [21]. Both these theoretical results, though on the higher side of the experimental data, are within the error limit of 17% in the measurements of Tarnovsky et al. [28] and Baiocchi et al. [29]. The C–H bond lengths in these radicals and in the CH_4 molecule are nearly the same, hence the peak Q_{ion} magnitudes are dependent on the respective ionization potentials. All the reactive radicals CH_x considered in this work have in common a peculiar property that, their bond lengths C–H

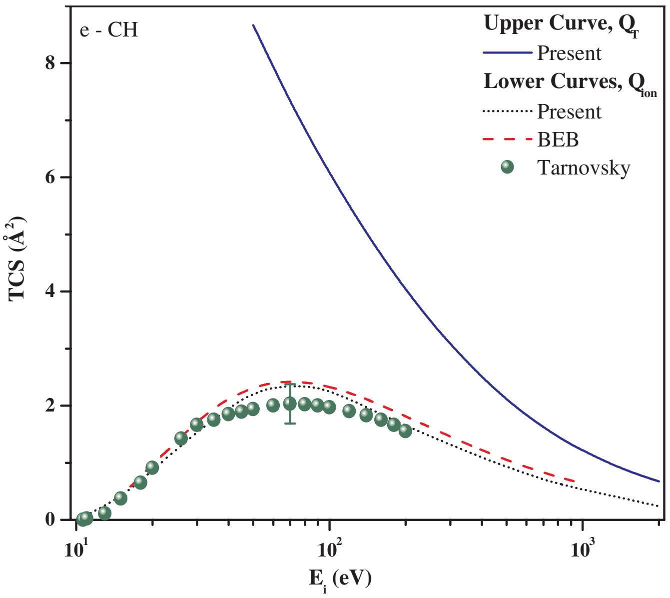

Fig. 9. Q_T and Q_{ion} for CH. $Q_T \rightarrow$ solid curve – present. $Q_{ion} \rightarrow$ dotted curve – present; dash – BEB [21]; circle – Tarnovsky [28].

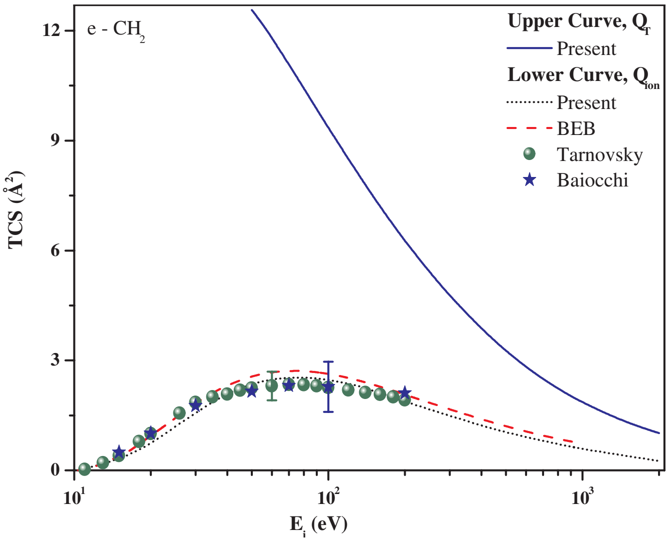

Fig. 10. Q_T and Q_{ion} for CH_2. $Q_T \rightarrow$ solid curve – present. $Q_{ion} \rightarrow$ dotted curve – present; dash – BEB [21]; circle – Tarnovsky [28]; star – Baiocchi [29].

are almost similar to that of their parent molecule CH_4, but have the ionization thresholds lower than their parents [30]. Therefore, the relative magnitudes of the present Q_{ion} for the radicals and their parent molecule, appear to be consistent here. The radicals show a dominant dipole rotation at lower energies.

4 Conclusions

The Complex scattering potential-ionization contribution, CSP-ic method developed by us recently has been applied

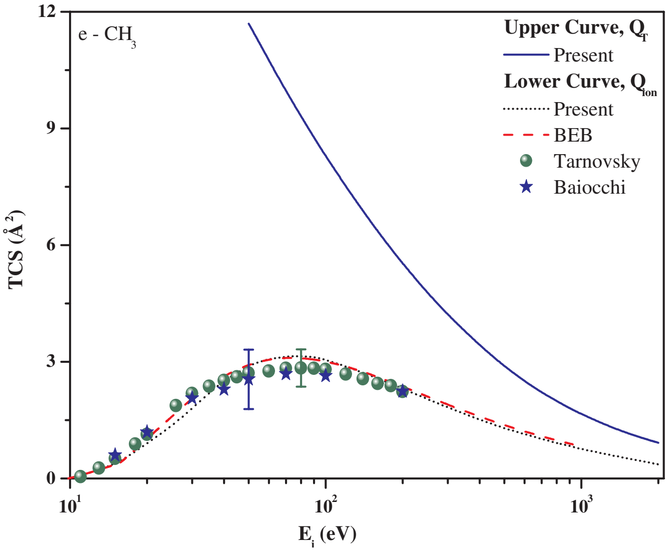

Fig. 11. Q_T and Q_{ion} for CH_3. $Q_T \rightarrow$ solid curve – present. $Q_{ion} \rightarrow$ dotted curve – present; dash – BEB [21]; circle – Tarnovsky [28]; star – Baiocchi [29].

to calculate Q_{ion} for CH_x radicals and other stable hydrocarbon molecules. To find the electron impact Q_T we have used the established SCOP method on these targets. We note that in view of the approximations made here no definitive values are claimed, but by and large our results fall within experimental error limits in many cases.

The present calculated results are compared with available data. By and large, our theoretical results on the stable molecular hydrides show satisfactory agreement with other theoretical and experimental investigations. The present Q_T for hydrocarbons including the tetrahedral CH_4 show reasonable agreement with various experimental data. Such calculations for reactive radicals (CH_x) now provide a first estimate of Q_T where no other data is available. Similarly Q_{ion} for C_3H_4 has not been investigated yet, hence the present calculations are important. In all the other targets studied here, present Q_{ion} find good comparison with available data

For the transient radicals, since the ionization threshold is lower, peak values of Q_{ion} are found to be higher and they occur at relatively lower energies as compared to the parent stable molecule, CH_4. This is evident from Table 2. In case of CH_x, the agreement of the present theory with the previous measurements and theories is found to be quite satisfactory.

The present method successfully employed here for many targets (CH_4, C_2H_2, C_2H_4, C_2H_6, C_3H_4, C_3H_6, C_3H_8 molecules and CH_x radicals), provides a reasonable estimate of ionization in relation to electronic excitations and also elastic cross-section.

MV thanks Prof. N.J. Mason, Department of Physics and Astronomy, Open University, Milton Keynes, UK and Royal Society Fellowship at UK during the tenure of this research. BKA thanks Council of Scientific & Industrial Research, India under which the present work was partly carried out. This research was funded in part by a project awarded to KNJ by Indian Space Research Organization, (Banglore) India.

References

1. H. Tawara, R.A. Phaneuf, Comm. At. Mol. Phys. **11**, 177 (1988)
2. *Concise Encyclopedia of Science and Technology*, edited by P. Sybil (McGraw-Hill, New York, 1989)
3. J.J. Perry, Y.H. Kim, J.L. Fox, H.S. Porter, Geophys. Res. **104**, 16541 (1999)
4. G.P. Karwasz, R.S. Brusa, A. Zecca, Riv. Nuovo Cim. **24**, 1 (2001)
5. W.M. Ariyasinghe, D. Powers, Phys. Rev. A **66**, 052716 (2002)
6. S.L. Xing, Q.C. Shi, X.J. Chen, K.Z. Xu, B.X. Yang, S.L. Wu, R.F. Feng, Phys. Rev. A **51**, 414 (1995)
7. O. Sueoka, S. Mori, J. Phys. B: At. Mol. Opt. Phys. **22**, 963 (1989)
8. A. Jain, K.L. Baluja, Phys. Rev. A **45**, 202 (1992)
9. Y.K. Kim, M.A. Ali, M.E. Rudd, J. Res. NIST **102**, 693 (1997)
10. S.H. Zheng, S.K. Srivastava, J. Phys. B **29**, 3235 (1996)
11. A. Gaudin, R. Hagemann, J. Chem Phys. **64**, 1209 (1967)
12. M. Hayashi, *Electron collision cross-sections determined from beam and swarm data by Boltzmann analysis* in *Nonequilibrium Processes in Partially Ionized Gases*, edited by M. Capitelli, J.N. Bardsley (Plenum Press, New York, 1990)
13. O. Sueoka, S. Mori, J. Phys. B: At. Mol. Phys. **19**, 4035 (1986)
14. Y. Jiang, J. Sun, L. Wan, Phys. Rev. A **52**, 398 (1995)
15. D. Rapp, P. Englander-Golden, J. Chem. Phys. **43**, 1464 (1965)
16. H. Nishimura, H. Tawara, J. Phys. B **27**, 2063 (1994)
17. W. Hwang, Y.K. Kim, M.E. Rudd, J. Chem. Phys. **104**, 2956 (1996)
18. M. Hayashi, Electron collision cross-sections for molecules determined from beam and swarm data, in *Swarm Studies and Inelastic Electron-Molecule Collisions*, edited by L.C. Pitchford, B.V. McKoy, A. Chutjian, S. Trajmar (Springer-Verlag, New York, 1987)
19. H. Chatham, D. Hills, R. Robertson, A. Gallagher, J. Chem. Phys. **81**, 1770 (1984)
20. B.L. Schram, M.J. van der Wiel, F.J. de Heer, H.R. Moustafa, J. Chem. Phys. **44**, 49 (1966)
21. Y.K. Kim, Web site: `physics.nist.gov/PhysRefData/Ionization`
22. C. Makochekanwa, H. Kawate, O. Sueoka, M. Kimura, M. Kitajima, M. Hoshino, H. Takaka, Chem. Phys. Lett. **368**, 82 (2003)
23. C. Szmytkowski, S. Kwitnewski, J. Phys. B: At. Mol. Opt. Phys. **35**, 3781 (2002)
24. K. Floeder, D. Fromme, W. Raith, A. Schwab, G. Sinapius, J. Phys. B: At. Mol. Opt. Phys. **18**, 3347 (1985)
25. H. Nishimura, H. Tawara, J. Phys. B: At. Mol. Opt. Phys. **24**, L-363 (1991)
26. H. Deutsch, K. Becker, R.K. Janev, M. Probst, T.D. Märk, J. Phys. B: At. Mol. Opt. Phys. **33**, L865 (2000)
27. H. Tanaka, Y. Tachibana, M. Kitajima, Phys. Rev. A **59**, 2006 (1999)
28. V. Tarnovsky, A. Levin, H. Deustch, K. Becker, J. Phys. B: At. Mol. Opt. Phys. **29**, 139 (1996)
29. F.A. Baiocchi, R.C. Wetzel, R.S. Freund, Phys. Rev. Lett. **53**, 771 (1984)
30. K.N. Joshipura, M. Vinodkumar, U.M. Patel, J. Phys. B: At. Mol. Opt. Phys. **34**, 509 (2001)
31. K.N. Joshipura, B.K. Antony, V. Minaxi, J. Phys. B: At. Mol. Opt. Phys. **35**, 4211 (2002)
32. K.N. Joshipura, M. Vinodkumar, B.K. Antony, N.J. Mason, Eur. Phys. J. D **23**, 81 (2003)
33. K.N. Joshipura, M. Vinodkumar, C.G. Limbachiya, B.K. Antony, Phys. Rev. A **69**, 022705 (2004)
34. B.K. Antony, K.N. Joshipura, N.J. Mason, Int. J. Mass Spectrom. **233**, 207 (2004)
35. K.N. Joshipura, B.K. Antony, Phys. Lett. A **289**, 323 (2001)
36. K.N. Joshipura, C.G. Limbachiya, Int. J. Mass Spectrom, **216**, 239 (2002)
37. D. Staszewska, D.W. Schwenke, D. Thirumalai, D.G. Truhlar, Phys. Rev. A **29**, 3078 (1984)
38. J.E. Turner, H.G. Paretzke, R.N. Hemm, H.A. Wright, R.H. Ritchie, Radiat. Res. **92**, 47 (1982)
39. M.A. Ali, Y.-K. Kim, W. Hwang, N.M. Weinberger, M.E. Rudd, J. Chem Phys. **106**, 9602 (1997)
40. W.M. Huo, V. Tarnovsky, K.H. Becker, Chem. Phys. Lett. **358**, 328 (2002)
41. H. Deutsch, K. Becker, S. Matt, T.D. Märk, Int. J. Mass Spectrom. **197**, 37 (2000), and references therein
42. A. Zecca, G.P. Karwasz, R.S. Brusa, C. Szmytkowski, J. Phys. B **24**, 2747 (1991)
43. M.-T. Lee, I. Iga, L.E. Machado, L.M. Brescansin, Phys. Rev. A **62**, 062710 (2000)
44. K.N. Joshipura, M. Vinodkumar, Z. Phys. D **41**, 133 (1997)
45. B.K. Antony, K.N. Joshipura, N.J. Mason, J. Phys. B: At. Mol. Opt. Phys. **38**, 189 (2005)
46. I. Iga, M.-T. Lee, P. Rawat, L.M. Brescansin, L.E. Machado, Eur. Phys. J. D **31**, 45 (2004)
47. L.M. Brescansin, P. Rawat, I. Iga, M.G.P. Homen, M.-T. Lee, L.E. Machado, J. Phys. B: At. Mol. Opt. Phys. **37**, 471 (2004)
48. R. Panajotovic, M. Kitajima, H. Tanaka, M. Jelisavcic, J. Lower, L. Campbell, M.J. Brunger, S. Buckman, J. Phys. B: At. Mol. Opt. Phys. **36**, 1615 (2003)